RSC Advances




ROYAL SOCIETY OF CHEMISTRY

www.rsc.org/advances

# Improved cell infiltration and vascularization of three-dimensional bacterial cellulose nanofibrous scaffolds by template biosynthesis

Zhe Li[a,Ψ], Xiangguo LV[b,Ψ], Shiyan Chen[a]*, Baoxiu Wang[a],

Chao Feng[b]*, Yuemin Xu[b], Huaping Wang [a]*

[a] State Key Laboratory for Modification of Chemical Fibers and Polymer Materials, Key Laboratory of Textile Science & Technology (Ministry of Education), College of Materials Science and Engineering, Donghua University, Shanghai, 201620, People's Republic of China

E-mail: chensy@dhu.edu.cn, wanghp@dhu.edu.cn

Tel: +86-21-67792958, fax: +86-21-67792950

[b]Department of Urology, Affiliated Sixth People's Hospital, Shanghai Jiaotong University, Shanghai, 200233, People's Republic of China

E-mail: engchaomed@sina.com

Tel: +86-21-64369181, fax: 86-21-64083783

[Ψ]Co-first author: These authors contributed equally to the work.

**Abstract**

A significant problem limiting the application of bacterial cellulose (BC) nanofibrous scaffolds for tissue regeneration is the nanoscale pores that inhibit cell infiltration and vascularization in their three-dimensional (3D) structure. In this paper, a facile method was used to fabricate 3D microporous nanofibrous Gelatin/BC composite scaffolds (Gel/BC) by stationary cultivation *Gluconacetobacter xylinus* using microporous gelatin scaffold as a template. The Gel/BC scaffolds with highly interconnected micropore (171 ± 71 μm) and surface decorated on the micropore walls by BC nanofibers (25.2 ± 7.0 nm) were fabricated, which are remarkably similar in structure to the native extracellular matrix (ECM). Cell distribution, viability and morphology were evaluated by seeding adipose-derived stem cells (ADSCs) on the scaffolds, using the 3D laser scanning confocal microscopy (3D-LSCM), LIVE/DEAD® viability/cytotoxicity assay and field emission scanning electron microscopy (FE-SEM). *In vivo* biocompatibility was evaluated by subcutaneous implantation using a dog model for 2 weeks. These results indicate that the 3D microporous nanofibrous scaffolds exhibit good biocompatibility, promoting cellular attachment, proliferation and maintain cellular phenotype, improving cellular infiltration and vascularization. It is anticipated that this 3D microporous nanofibrous scaffold can be applied in the fields such as medical implants, cell supports, and materials, which can be used as instructive 3D environments for tissue regeneration.

**Keywords:** Bacterial cellulose; Nanofibers; Microporous; Template biosynthesis; Tissue regeneration

## 1. Introduction

The final goal in tissue engineering scaffold is to biomimetic the cell microenvironment *in vivo*. Cells are inherently sensitive to their three-dimensional (3D) environments from the macroscale, microscale, to the nanoscale.[1] The nanoscale structure of the extracellular matrix (ECM) provides a natural network of nanofibers (30~100 nm) to support cells and guide their behavior. It has been proved that the nanofibrous materials which resemble the architecture of ECM can influence cell-material interaction and promote cell behaviors such as attachment, proliferation and expression of matrix components.[2-4] Moreover, an essential requirement for tissue regeneration is the microporous architecture in 3D with appropriate pore sizes (100~400 μm) and porosities (~90 %) to support cell migration, proliferation, vascularization and tissue ingrowth[5]. Therefore, a key challenge of tissue engineering is the design and fabrication of the 3D highly porous nanofibrous scaffolds that exhibit multi-scale structures composed of microporous structure with nanofibers for more biomimetic cellular environment.[6, 7]

Although several strategies, including multi-layer sintering,[8] liquid-assisted collection,[9] adding porogen[10] and hybrid nano-/microfiber,[11] have been performed to prepare highly porous nanofibrous scaffolds, none of these methods provides access to obtain ideal scaffolds mimicking the ECM structure with simple processes and tunable architectures. Bacterial cellulose (BC) has recently received extensive attention as excellent nanofibrous scaffolds candidating for tissue regeneration benefit

from their refined 3D nanofibrils network architecture which successfully mimics the native ECM.[12] Meanwhile, it possesses desirable physical and mechanical properties, such as high mechanical strength, mouldability, biocompatibility and unique nanostructure, much interest has been given on the development of medical applications for artificial skins,[13] blood vessels,[14] bone,[15] cartilage,[16] meniscus,[17] urinary[18] and tympanic membrane[19]. However, the relatively dense nanostructure of the nanofibrous network possess only small pore size (less than 5 μm), which inhibit cell infiltration, migration, ingrowth and vascularization.[20]

Different methods for fabricating 3D high porous BC scaffolds have been reported. Among these, one of most applied method is the employing starch, paraffin and agarose as porogen in the fermentaion process.[21-23] However, this method can only produce porous membranes with poor interconnectivity for the pore, less mechanical strength and might contain residual solvent and/or porogens.[24] Hence, to avoid these problems, the BC pellicles is homogenized to slurry of individual fibrils which are combined with soluble polysaccharide.[25-27] After cross-linking and freeze-drying, the composite sponges with high porous interconnectivity are fabricated. Those studies indicated the pore sizes, porosity, interconnectivity and macro shapes of the resultant scaffolds can be tailored by altering the concentration, freezing temperature and mold shapes.[28] However, this method disrupts the native 3D network structure of BC that are less similar in structure to ECM. More significantly, amount of individualized cellulose nanofibrils are integrated by polysaccharide as

glue, which results in low surface area and nanoscale surface roughness of the pore walls, to further influence cell-material interaction.

In this paper, a novel and simple method was developed to fabricate BC composite scaffolds with 3D microporous and nanofibrous structure by stationary cultivation *Gluconacetobacter xylinus* using microporous gelatin scaffold as template. The template was prepared by freeze-drying, which makes it possible to control the resulting microporous size and interconnectivity. The morphology and structural characteristics of the resulting Gelatin/BC composite scaffolds (Gel/BC) were investigated by FE-SEM, XRD and ATR-FTIR. Adipose-derived stem cells (ADSCs) were cultured in the scaffolds. Cell viability, proliferation and morphology were investigated *in vitro* to evaluate the cytocompatibility, cell attachment and infiltration. Furthermore, the biocompatibility *in vivo* was evaluated by subcutaneous implantation using a dog model for 2 weeks.

## 2. Materials and methods

### 2.1. Materials

*Gluconacetobacter xylinus* strain 1.1812 was obtained from Institute of Microbiology, Chinese Academy of Science. All chemicals were purchased from Sinopharm Chemical Reagent Co., Ltd. (China). Ultrapure water (endotoxin free water) from the MilliQ system and 0.45 μm cellulose ester filtration membranes were obtained from Millipore Co. (Billerica, USA), and used in all the experiments. The culture medium for *Gluconacetobacter xylinus* was used: 5.0 wt% D-glucose, 0.5

wt% peptone, 0.5 wt% yeast extract, 0.2 wt% disodium hydrogen phosphate, 0.1wt% monopotassium phosphate and 0.1 wt% citric acid, the pH was adjusted to 5.0 with NaOH. The medium were sterilized at 121 $^{o}$C in autoclave for 30 min by autoclaving.

2.2. Template biosynthesis of Gel/BC nanocomposites

Gelatin was hydrated in ultrapure water at concentraions of 2 wt%, and incubated at 37 $^{o}$C for 1h with constant stirring. After that, the gelatin solution was poured into a sqare polyterafluoroethylene (PTFE) mold and frozen at -20 $^{o}$C for 12h. The frozen sample in the mold was lyophilized for 24 h to prepare a 3D microporous scaffold and stored at 4 $^{o}$C until further usage.[29] The gelatin scaffolds were cross-linked with 2% (w/w) glutaraldehyde solution for 10 min, followed by washing with ultrapure water. Then, the microporous scaffolds were disinfected with 75 wt% ethyl alcohol for 1 h at room temperature and rinsed with the culture medium for 3 times. The culture medium was lightly squeezed out and sucked into sterilized filer paper. About 40 mL bacterial suspensions in the culture medium with initial bacterial density of $3.8\times10^{5}$ cells/mL were seeded on the gelatin scaffolds. The surface of gelatin scaffolds were covered with a oxygen permeable silicone sheet (thichkness: 100 μm). The mixed compound were incubated statically at 30 $^{o}$C, for 7 days to produce Gel/BC composite scaffolds. To further purification, the composites were immersed in 75 wt% ethyl alcohol for 24 h, and subsequently treated with 1 wt% Triton X-100 in ultrapure water for 24 h, then rinsed with a large amount of ultrapure water for 3 times to remove the excess chemical.[30] The Gel/BC composite samples

were lyophilized for 24 h to obtained 3D microporous nanofibrous scaffolds and stored at 4 $^{o}$C until further usage.

2.3. Endotoxin analysis

The resulting Gel/BC scaffolds was analyzed by bacterial endotoxin testing using Gel-Clot Limulus Amebocyte Lysate (LAL) kit with the sensitivity of 0.5 EU/mL. Gel-clot assay is a qualitative assay providing a simple positive/negative result, has been cited in Chinese Pharmacopeia.[31] Samples was immersed in endotoxin-free water with the ratio of 0.1 g of sample/mL. The extraction was done at 37 $^{o}$C for 2h under orbital motion at 160rpm. Then, the endotoxin extraction was incubated with LAL at 37 $^{o}$C for 1h. After proper incubation, a firm and intact gel withstands 180$^{o}$ inversion indicated positive result for the presence of endotoxin.

2.4. Morphology and structure characterization

The morphology of the samples was characterized by field emission scanning electron microscopy (FE-SEM). The pure BC, gelatin template and Gel/BC scaffold were cut into small pieces and coated with a thin layer of evaporated gold and observed with a Hitachi S-4800 (Hitachi, Japan). From the FE-SEM images, the distributions of micropore size and nanofiber diameter were obtained by ImageJ software (n = 200). The attenuated total reflection Fourier transform infrared (ATR-FTIR) spectra of samples were measued with a Nicolet NEXUS-670 (Nicolet,

USA) instrument in the absorption mode with the wave number range of 4000-600 $cm^{-1}$. X-ray diffraction (XRD) patterns was carried out on the freeze-dried samples in reflection mode ($2\theta$ = 5-80$^{o}$) using a D/Max-2550 PC (Rigaku, Japan) with Cu Kα radiation generated at 40 kV and 30 mA. The wet state mechanical property of the samples was detemined by measuring the tensile strength of scaffolds using an Instron 5969 Double Column Universal Tesing System (Instron, USA) equipped with a 100 N loading cell. The samples were trimmed into rectangular disks of 60 × 20 × 5 $mm^3$, and a constant crosshead displacement rate of 5 mm/min was used. All measurements were performed in distilled water at 37 $^{o}$C. Each sample was repeated for three times to take the average values.

2.5. Cellular evaluation *in vitro*

Adipose tissue was obtained from the inguinal regions of adult healthy beagle dogs. The experimental protocol was approved by the Research Ethical Committee of Shanghai 6th People's Hospital. The isolation and culture of adipose-derived stem cells (ADSCs) were performed as previously described.[32] Brifefly, the adipose tissues were washed thoroughly with 0.25 % chloramphenicol solution and phosphate buffer saline (PBS, pH = 7.4) three times, then digested with 0.01 % collagenase I for 1 h at 37 $^{o}$C. Enzymatic activity was stopped by adding Dulbecco's modified Eagle's medium (DMEM) supplemented with 10 % fetal bovine serum (FBS). The above solution was further filtered with a 50 μm mesh filter to remove the undigested tissue and then centrifuged at 1000 rpm for 10 min. The cell pellet was resuspended and

cultured in the growth medium by DMEM with 10% FBS and cultured at 37 $^{o}$C with 95 % humidity and 5 % $CO_2$. These cultured cells were referred as P0 cells. The characterization of ADSCs was determined by CD 90, CD 44, CD 105 and CD 34 antibody. After culturing for 3-5 days, the cell colonies reached 70-80 % confluence and were then passaged with 0.05 % trypsin-EDTA (Gibco, USA). ADSCs of passage 2 were used for the study.

ADSCs suspended in the medium were seeded onto the scaffold surface of Gel/BC (10×10 mm) at a density of $10^4$ cells/mL and cultured for 14 days, with the growth medium being changed every day. We determined ADSCs distribution and viability during growth on the scaffolds using the LIVE/DEAD® viability/cytotoxicity assay by laser scanning confocal microscopy (LSCM, Carl Zeiss, LSM710). After cell cultivation for 1 day, 7 days and 14 days, we rinsed scaffolds twice with Dulbecco's phosphate buffered saline (DPBS). 500 μL of the combined LIVE/DEAD® assay reagents (4 μM of EthD-1 and 2 μM of calcein AM in DPBS) was added to the scaffold surfaces, incubated for 45 min at 25 $^{o}$C and imaged the labeled cells using a LSCM. Viable cells labeled with calcein AM were detected at an excitation wavelength of 494 nm. Dead cells labeled with EthD-1 were detected at an excitation wavelength of 528 nm. A z-step of 0.2 mm was used to optically section the samples. Observations with 20 × oil immersion lenses were performed. Data files were saved in tiff format and processed with Image J Software. Cell viability and the total percentage of viable cells were determined by counting live and dead cells (n=2000 cells) for each growth condition. The proliferative capacity of ADSCs in Gel/BC

scaffolds were determined by the alamar blue assay kit (Invitrogen).[23] After cell cultivation for 1 day, 3 days, 7 days and 14 days, four randomly chosen cells seeded scaffolds from each group were cut into squares with a surface area of 0.2cm$^2$, washed twice with PBS, incubated with alamar blue solution for 5 h at 37 $^{o}$C. Then fluoresence was measured at absorbable wavelengths of 570 and 600 nm. To compare the differences of cells viability and proliferation on pure BC, Gelatin template and Gel/BC scaffolds, we performed chi-squared tests. We considered a *P*-value < 0.05 to indicate statistically significant data.

Cell adhesion onto scaffolds were evaluated by FE-SEM. Briefly, ADSCs suspended in the medium were seeded onto the surface of scaffolds (10 × 10 mm) at a density of $10^4$ cells/mL and cultured for 24 h. Then the samples were rinsed twice with DPBS and fixed in a solution of 2.5% glutaraldehyde and 1% osmium tetroxide in PBS, and dehydrated in graded ethanol (50–100%). Before examination, they were dried using supercritical carbon dioxide extraction and then coated with gold and thereafter examined with a Hitachi S-4800 (Hitachi, Japan).

2.6. *In vivo* implantation

General anesthesia was induced by intravenous injection of pentobarbital. The back skin of the dogs was shaved and disinfected with 75 % ethanol. A 2 cm long incision was made . The pure BC, gelatin template and Gel/BC scaffolds were then subcutaneously implanted into 1 year old female dogs (n=5). Before closing the skin , silk sutures fixed those flat samples in each corner as the operative marker. The grafts

were harvested 2 weeks after implantation, fixed in 10 % neutral buffered formalin, dehydrated and embedded in paraffin. Cross sections (5 μm) were cut and stained with hematoxylin and eosin stainin (H&E). Masson's trichrome staining was carried out to assess the collagen deposition. Immunohistochemical staining with the platelet endothelial cell adhesion molecule (PECAM-1, CD 31) to detect vascularization, T-cell specific antibody (CD 3), B-cell specific antibody (CD 22) and macrophage-specific antibody (CD 68) were also used to identify the severity and type of inflammation.

## 3. Results and discussion

### 3.1. Template Synthesis of 3D microporous nanofibrous scaffolds

Schematic illustration of template synthesis of Gel/BC nanocomposites is outlined in Fig. 1. Gelatin is a natural polymer which is derived from collagen, with the excellent biocompatibilty and biodegradable, it has been widely used in the constructing the tissue reconstruction biomaterial.[33] The microporous gelatin scaffolds can be facilely obtained by freeze-drying, and the pore architecture of the scaffolds can be controlled by varying the freezing temperature and concentration of gelatin solution.[29] Firstly, the relationship between the concentraion and pore size is established by freeze-drying the gelatin solution at 20 $^{o}$C, which could provide supporting parameter for preparation of porous template with the appropriate pore sizes and porosity. In our study, we selected the microporous gelatin template with the

mean diameter about 200 μm, which conform to the architecture requirement of tissue regeneration.[5] As shown in Fig. 1a, b, gelatin template is a white porous sponge with a three-dimensionally open porous and interconnected network structure. When the gelatin scaffold was immersed into bacterial suspensions, all of those bacteria were readily impregnated into the interconnected networks. After that these bacteria intimately adhered onto the inside wall of gelatin micropore, and then BC nanofibers were biosynthesized by *Gluconacetobacter xylinus* (Fig. 1c). The BC nanofibers only can be synthesizd in the presence of oxygen and culture medium, the high porosity and interconnectivity of the gelatin scaffolds allowed adequate supply of oxygen and nutrient diffusion into the matrix.[34] Meanwhile, the high density of hydroxyl groups on the surface of the nanofibers can form hydrogen bonding with amide groups of gelatin.[35] Therefore, driven by the hydrogen bonds and vander Waals forces, the good interfacial adhesion and interactions created between BC nanofibers and the pore wall surface of the gelatin. In this study, we also used a mild purified process attempting to retain the original microporous architecture of gelatin scaffolds and remove endotoxins from the Gel/BC scffolds (Fig. 1a and d). The Gel-clot assay showed a negative result, indicating the endotoxin level is less than 0.5 EU/ml. This value was below the endotoxin limit (0.5 EU/mL or 20 EU/device) set by the USA Food and Drug Administration (FDA) for medical devices. Finally, a 3D microporous nanofibrous scaffolds of Gel/BC with high microporous and cellulose nanofibers was fabricated by template biosynthesis method. More significantly, this method as a platform technology makes it possible to design and fabricate 3D composite scaffolds

with defined macro-, micro- and nanostructure length scales, which would better mimic the natural hierarchical organization of ECM.

3.2. Morphology and structural characteristics

BC is synthesized by *Gluconacetobacter xylinus* in a static liquid culture medium. During the process of this biosynthesis, the nutrition medium are utilized by the bacteria and glucose molecules are polymerized into linear β-1,4-glucan chains. The linear glucan chains aggregated into fibrils that are then assembled and crystallized into hierarchically composed ribbons. A gelatinous BC pellicle, consists of the ultrafine ribbons with diameter of less than 100 nm, is deposited layer by layer at the air-medium interface with thickness increasing over time.[12] As shown in Fig. 2a, the cross-section morphology of the native BC pellicle exhibits a multilayer asymmetric structure with the compact side that is biosynthesized at the air-media interface denser than the medium-facing side (porous side).[36] High magnification of the cross-section morphology at the porous side of BC is shown in Fig. 2a inset, which exhibited a 3D homogeneous and interconnected porous structure composed of nanofibrous networks with the pore size about 5 μm. The details of the surface at the compact side are shown in Fig. 2b, which exhibits 3D and interconnected network structure of long cellulose nanofiber with a high aspect ratio and fiber diameter is 23 ± 6.1 nm (Fig. 2c). The nanoscale structure of BC entangled nanofibrous network is similar to collagen fibrils found in the native ECM, with high tensile strength.[37] This provides the possibility of mimicking the ECM microenvironment by using the

unique and desirable structure of BC. However, the cross-section and surface morphology of BC also displayed a dense network of nanofibrous, which resisted cellular penetration and prohibits cells from establishing cell-cell contact in three dimensions.[23]

As shown in Fig. 3, the cross-section morphology of the gelatin template and Gel/BC scaffold with different magnifications were revealed by FE-SEM observation, and the distributions of micropore size and nanofiber diameter were obtained from the FE-SEM images. We selected the collagen-derived gelatin as a porous template, because of its excellent biocompatibilty and biodegradability. It can be readily obtained by freezing and lyophilizing methods and various porous structures including pore size and distribution can also be tailored by adjustment of the mass fraction and process parameters. In our study, the gelatin template is comprised by open and interconnected micropore, and the pore wall surface is smooth and no nanofibrous architechure (Fig. 3a and b). Furthermore, the average micropore diameter was determined to be 179 ± 69 μm (Fig. 3c), indicating their suitability for scaffolding cells. The Gel/BC scaffold with 3D microporous nanofibrous structure was prepared by forming BC nanofibrous network in the opentings of microporous gelatin template. The existence of the template renders the composite scaffold to maintain desirable shape on a large scale as observed by the digital photographs (Fig. 1a and d) with the same thickness(about 6 mm). The FE-SEM image shown in Fig. 3d gives an overview of microscale topography of the Gel/BC composite scaffold, which suggests the maintain of open micropore with a high degree of interconnectivity.

Moreover, the microscale pores show nanoscale roughness, which improved the biological performance (Fig. 3e). It is worth noting that the micropore diameter of Gel/BC scaffold slightly decreases to 171 ± 71 μm (Fig. 3f), which is consistent with the pore size of the gelatin template (179 ± 69 μm). Under higher magnification, micropore of Gel/BC scaffold as shown in Fig. 3g exhibited the unique BC nanofibrous network which uniformly distributed on the gelatin matrix, further demonstrating the remarkable nanoscale surface roughness. The 3D non-woven nanofibrous architecture of BC show close resemblance to the ECM, and the average nanofiber diameter is 25.2 ± 7.0 nm (Fig. 3h and i). It has been reported that the nanoscale fibers and high porous structure can significantly influence the cell-material interaction and cell behavior.[38, 39] In this work, a 3D microporous nanofibrous scaffold can be designed and fabricated by the template biosynthesis method, which retaining the macro shapes (such as ear-like or tube-like shapes) and microporous architecture from the template scaffold, and introducing nanoscale roughness on the scaffold pore walls caused by BC nanofibers.

### 3.3. ATR-FTIR and XRD characterization

Fig. 4a shows the ATR-FTIR spectra of the pure BC, gelatin template and Gel/BC scaffold at wave numbers ranging from 4000 to 650 $cm^{-1}$. The characteristic peaks of cellulose locate at 3347, 2910, 1644, 1372, 1162 and 1060 $cm^{-1}$ in the spectrum of BC. The strong absorption at 3347 $cm^{-1}$ can be identified as the hydroxyl group (-OH) stretching vibration, whereas absorption at 2910 $cm^{-1}$ demonstrates the

presence of the stretching vibration of the $CH_2$ bond. The band around 1644 $cm^{-1}$ comes from the O-H bending vibration, which demonstrates the occurrence of combined micro amount of water in BC. The peaks at 1372 $cm^{-1}$, 1162 $cm^{-1}$ and 1060 $cm^{-1}$ represents C-H bending vibration, C-O-C and C-O stretching vibration. For the gelatin scaffold, the characteristic absorption bands at 3297, 1634, 1544, and 1239 $cm^{-1}$ represents the combination of O-H and N-H stretching vibrations, amide I, II, and III bands, respectively. The spectrum of the Gel/BC composite demonstrated that all these characteristic bands of BC and gelatin could be observed with a slight shift of their location. Furthermore, the amide I band with a characteristic frequency of 1634 $cm^{-1}$ is associated with the stretching vibrations on C=O groups along the polypeptide backbone and is a sensitive marker of polypeptide secondary structure. It is noted that the absorbance of amide I band red shift at 1651 $cm^{-1}$ in the spectrum of the Gel/BC composite compared to the band at 1644 $cm^{-1}$ in the spectrum of BC. This confirms that some hydrogen bonds formed in the ordered region of amide I band, suggesting the formation of the interaction between BC and gelatin. The FTIR observation indicates that the Gel/BC nanocomposites has been successfully made by using the template biosynthesis method. The XRD patterns of BC, Gel/BC composites and pure gelatin are shown in Fig. 4b. The pure BC exhibits three typical diffraction peaks at about 14.4°, 16.7° and 22.6°, which are attributed to the presence of crystalline cellulose I from BC, corresponding to $(1\bar{1}0)$, (110), and (200) planes.[40] The profile of gelatin shows a broad peak in the $2\theta$ range of 15-25°, meanwhile no sharp peak is observed, which is a typical XRD pattern of pure gelatin. For the Gel/BC

composite, the very weak characteristic peaks of BC and the characteristic broad diffraction peak of gelatin are showed. It suggests that the BC nanofibers coating can be formed and enwrap the surface of 3D microporous gelatin scaffold, which is consistent with the FE-SEM and FTIR results.

3.4. Mechanical properties

To characterize the mechanical properties, tensile strength and elastic modulus were determined at 37 $^{o}$C in distilled water. The values of stress at break, strain at break and Young's modulus of pure BC, gelatin template and Gel/BC composites are demonstrated in Fig. 5a. Undoubtedly, pure BC shows an excellent wet state mechanical property, the tensile stress can reach to 650.2 ± 25.3 kPa, the strain and Young's modulus are up to 20.0 ± 2.8 % and 3.25 ± 0.30 MPa, respectively. The result can be explained by the unique dense nanofibrous network structure and high crystallinity of BC. On the other hand, the Young's modulus of Gel/BC composites is measured to be 1.29 ± 0.11 MPa, 8.6 folders higher than the gelatin template, 0.15 ± 0.04 MPa. The stress at break is 191.4 ± 15.3 kPa, about 8 folders greater for the peak stress of pure gelatin template (23.6 ± 5.9 kPa). Furthermore, the typical tensile stress-strain curves for Gel/BC and gelatin template are shown in Fig. 5b, indicate a significantly improved mechanical performance for the microporous template scaffolds reinfored with nanofibrous network of BC. The BC content of the Gel/BC scaffold is less than 6 wt%, which is evaluated by immersing the sample in NaOH solution. In a previous study, different amounts of dried cellulose microfibers were

mixed with crosslinked gelatin solution and freeze-dried to fabricate 3D porous sponge scaffold. The mechanical property of our Gel/BC scaffold in wet state was comparable to that of the sample with 75 % cellulose microfibers in dried state.[25] In our study, small amount of BC with the native nanofibrils network structure is coated on the pore wall surface of gelatin matrix. The reinforcing effects of the BC network seem to be more efficient than adding individualized BC nanofibrils.[27] BC is a highly hydrophilic nanofibrous material with large surface area and excellent mechanical property,[41, 42] which allows extensive hydrogen bond formation with another hydrophilic polymer like gelatin.[43] Therefore, driven by the hydrogen bonds and vander Waals forces, the good interfacial adhesion and strong interactions created between BC and gelatin matrix result in a strong nanocomposite material.

3.5. Cellular evaluation *in vitro*

*In vitro*, scaffolding functions were evaluated in terms of cell viability, attachment and prolifertion. To investigate the cytotoxicity, we seeded ADSCs with a cellular density of $1.0 \times 10^4$ cells/mL onto the scaffolds and quantified the viability during 14 days cultivation. Based on the LIVE/DEAD® assay data (Fig. 6B), ADSCs grow on the three samples displayed a high viability (from 84 % to 91 %) over 14 days culture, there are no significantly differences among the scaffolds ($p > 0.05$). The results confirm that the cytocompatibility of Gel/BC is much comparable to gelatin and pure BC. The 3D distribution of ADSCs in scaffolds were observed after 1, 7 and 14 days cell culture (Fig. 6A). Direct observation of the ADSCs grow only on the

surface of pure BC, cells are unable to infiltrate inside the nanofibrous matrix. This can be explained that the average pore size of the dense network of BC is smaller than the physical dimensions of ADSCs. On the other hand, ADSCs can penetrate through and grow well in 3D culture of the gelatin template and Gel/BC scaffolds. When the freshly prepared ADSCs suspensions were seeded onto the surface of the microporous scaffolds, with average pore size about 170-180 μm, cells were allow to settle by gravity and infiltrate into the materials. The bottom of gelatin scaffolds have more cells accumulated, compared to the Gel/BC composites. The ADSCs distrubuted uniformly in the Gel/BC scaffolds, suggesting that the nanofibrous architecture of BC may enhance the attachment of cells against gravity. For cell proliferation in Fig. 6C, cultures on both pure BC and Gel/BC scaffolds show a rapid cellular growth during the first 72 h of culture, compared to the gelatin template, indicating that the nanofibrous network architecture provides a more favorable environment for initial cellular attachment. For the long-term cellular proliferation, a significant difference is found between Gel/BC scaffolds and the other two controls for the number of ADSCs 7 and 14 days after culture. The cell number of Gel/BC composites at the 14 days is measured to be $7.26 \times 10^5$ cells, about double higher than the gelain template ($3.68 \times 10^5$ cells), and 2.8 times higher than the pure BC ($2.57 \times 10^5$ cells), respectively. These results strongly demonstrated that the Gel/BC scaffolds with 3D microporous nanofibrous architecture provide a superior cell survival microenvironment for initial cell attachment, further cell proliferation and growth.

The microscopic morphology of ADSCs cultured on the scaffolds was observed by FE-SEM after 24 h culture, including nanofibrous membranes of pure BC, microporous scaffolds of gelatin, and 3D microporous nanofibrous scaffolds of Gel/BC. As shown in Fig. 7a and e, cells were attached to the surface and widely spead along the nanofibers, their abundant pseudopods tightly adhered to the nanofibers of BC and formed integrated cell-fiber constructs (Fig. 7e inset). Moreover, the ADSCs in these constructs exhibited wide cell-cell and cell-nanofibers contact, which was helpful for the maintenance of cell activity. As shown in Fig. 7d, the cell-nanofiber interaction can form between the cell-surface protein and hydroxyl groups of the BC nanofibers.[44] On the microporous scaffolds of gelatin scaffolds, cells show a flattened morphology and a small amount of cellular pseudopods were displayed, which randomly spread on the smooth surface wall of micropores (Fig. 7b and f). On the 3D microporous nanofibrous scaffolds of Gel/BC scaffolds, cells distributed in the micropores and anchored along the nanofibers of BC (Fig. 7c). The cells in Gel/BC scaffolds had a predominantly round morpholgy in this 3D culture, which clustered on the network of cellulose nanofibers with a spherical morphology (Fig. 7g). It was smaller in size than those cultured on BC nanofibrous membranes and smooth surface wall of micropores gelatin scaffold. Since the 3D microporous nanofibrous architecture structure is very similar to that of the extracellular matrix from natural tissue, the Gel/BC scaffolds may preserve the phenotype of ADSCs, predicting a maintainable bioactivity for cell survival support. These results are consistent with prevous finding that the 3D nanofibrous matrix used in long-term

cultures supported a higher cellular density with smaller cells than the 2D scaffold and selectively retained healthy, non-apoptotic cells.[45, 46]

3.6. *In vivo* biocompatibility of Gel/BC scaffolds

The *in vivo* biocompatibility of Gel/BC scaffolds was evaluated using a dog model in which pieces of pure BC, gelatin template and Gel/BC scaffolds were implanted subcutaneously, and harvested after 2 weeks. During the post-implantation, the implants could be palpated and found to be relatively soft and elastic. When harvesting at 2 weeks, the pure BC could easily be dissected from the adherent fibrous capsules, while the gelatin and Gel/BC scaffolds with no fibrous encapsulation were relatively difficult to separate it from the surrounding subcutaneous tissue. All the specimens took on a pink color, and no macroscopic signs of inflammation (i.e., redness, edema, or exudates) were observed around the implanted pieces or in the incision. For histological evaluation, H&E and Masson's trichrome staining were performed. It can be seen that only a few cells appeared in the pure BC, and the boundary is clear between BC and the tissue. Meanwhile, no boundary can be found between materials and tissue in the histological sections of gelatin and Gel/BC scaffolds. Fibroblasts grew into the inner pores of the material, and their size enlarged and quantity increased while collagen synthesis increased. The result of Masson staining showed that a substantial amount of callagen stroma was present within the inner of the gelatin and Gel/BC scaffolds, and no lymphocytes, neutrophils, granulocytes, or macrophages were prominent. Furthermore, the 3D microporous

nanofibrous scaffolds of Gel/BC showed a significant rapid vascularization *in vivo*. Ingrowing capillaries were coated with an inner endothelial layer. The cellular surface antigen CD 31 is a specific endothelial cell marker and suitable to quantify revascularization.[47, 48] In this study, immunostaining for CD 31 was used to monitor revascularization. The section of Gel/BC scaffolds labeling for CD 31 showed in blood vessels invading the scaffolds. The structure of Gel/BC scaffolds with 3D microporous nanofibrous architecture was well designed for revascularization, because the surface decorated material by cellulose nanofibers provided enormous surface area and connecting pores for the cells and for the ingrowth of blood vessels. Immunohistochemical staining of T-cell specific antibody (CD 3), B-cell specific antibody (CD 22) and macrophage-specific antibody (CD 68) was also used to identify the inflammatory cells. As shown in Fig. 8, only few inflammatory cells were found around the tissue, while the expression of CD 22 was found in all tissue. This can be attributed to the humoral immunity caused by mild infections, rather than the cellular immune response caused by reject reaction. Therefore, these results indicate that the Gel/BC scaffolds *in vivo* can facilitate cellular infiltration, ingrowth and neovascularization, with a mild inflammatory response and can be considered a good biocompatible material.

## 4. Conclusions

In conclusion, a facile and scalable method was used to fabricate 3D microporous nanofibrous composite scaffolds by stationary cultivation *Gluconacetobacter xylinus*

using microporous scaffolds as template. The template was prepared by freeze-drying, diverse macro shapes and various controllable micro-structures including pore size and distribution can be tailored by adjustment of the process parameters. During biosynthesis in the presence of microporous template, the cellulose nanofibers were decorated on the surface and internal of 3D microporous scaffolds. The resulting scaffolds can be systematically designed and fabricated with multiscale architecture, which are remarkably similar in structure to the natural hierarchical organization of native ECM. Furthermore, the *in vitro* and *in vivo* evaluation showed excellent biocompatibility, promote cell attachment, proliferation and maintain cell phenotypic, improved cell infiltration and vascularization in the 3D microporous nanofibrous scaffolds. It is anticipated that this 3D microporous nanofibrous scaffold can be applied in the fields such as medical implants, cell supports, and materials, which can be used as instructive 3D environments for tissue regeneration.

**Acknowledgements**

This work was supported by the National Natural Science Foundation of China (51573024, 51273043, 81370795 and 81100488) and the Fundamental Research Funds for Central Universities (CUSF-DH-D-2015029).

**References**

1. M. M. Stevens and J. H. George, *Science*, 2005, **310**, 1135-1138.
2. F. Yang, R. Murugan, S. Wang and S. Ramakrishna, *Biomaterials*, 2005, **26**, 2603-2610.

3. M. Schindler, I. Ahmed, J. Kamal, A. Nur-E-Kamal, T. H. Grafe, H. Y. Chung and S. Meiners, *Biomaterials*, 2005, **26**, 5624-5631.
4. X. Wang, B. Ding and B. Li, *Materials Today*, 2013, **16**, 229-241.
5. K. F. Leong, C. K. Chua, N. Sudarmadji and W. Y. Yeong, *Journal of the Mechanical Behavior of Biomedical Materials*, 2008, **1**, 140-152.
6. N. M. Alves, I. Pashkuleva, R. L. Reis and J. F. Mano, *Small*, 2010, **6**, 2208-2220.
7. S. I. Jeong, N. A. Burns, C. A. Bonino, I. K. Kwon, S. A. Khan and E. Alsberg, *Journal of Materials Chemistry B*, 2014, **2**, 8116-8122.
8. L. H. Leung, S. Fan and H. E. Naguib, *J Polym Sci Part B*, 2012, **50**, 242-249.
9. E. H. Gang, C. S. Ki, J. W. Kim, J. Lee, B. G. Cha, K. H. Lee and Y. H. Park, *Fibers and Polymers*, 2012, **13**, 685-691.
10. T. G. Kim, H. J. Chung and T. G. Park, *Acta Biomaterialia*, 2008, **4**, 1611-1619.
11. S. H. Park, T. G. Kim, H. C. Kim, D. Y. Yang and T. G. Park, *Acta Biomaterialia*, 2008, **4**, 1198-1207.
12. N. Petersen and P. Gatenholm, *Applied Microbiology and Biotechnology*, 2011, **91**, 1277-1286.
13. J. Kucińska-Lipka, I. Gubanska and H. Janik, *Polymer Bulletin*, 2015, **72**, 2399-2419.
14. A. Bodin, L. Ahrenstedt, H. Fink, H. Brumer, B. Risberg and P. Gatenholm, *Biomacromolecules*, 2007, **8**, 3697-3704.
15. S. Park, J. Park, I. Jo, S. P. Cho, D. Sung, S. Ryu, M. Park, K. A. Min, J. Kim, S. Hong, B. H. Hong and B. S. Kim, *Biomaterials*, 2015, **58**, 93-102.
16. A. Svensson, E. Nicklasson, T. Harrah, B. Panilaitis, D. L. Kaplan, M. Brittberg and P. Gatenholm, *Biomaterials*, 2005, **26**, 419-431.
17. A. Bodin, S. Concaro, M. Brittberg and P. Gatenholm, *Journal of Tissue Engineering and Regenerative Medicine*, 2007, **1**, 406-408.
18. A. Bodin, S. Bharadwaj, S. Wu, P. Gatenholm, A. Atala and Y. Zhang, *Biomaterials*, 2010, **31**, 8889-8901.
19. J. Kim, S. W. Kim, S. Park, K. T. Lim, H. Seonwoo, Y. Kim, B. H. Hong, Y. H. Choung and J. H. Chung, *Advanced Healthcare Materials*, 2013, **2**, 1525-1531.
20. F. V. Berti, C. R. Rambo, P. F. Dias and L. M. Porto, *Materials Science and Engineering C*, 2013, **33**, 4684-4691.
21. M. Zaborowska, A. Bodin, H. Bäckdahl, J. Popp, A. Goldstein and P. Gatenholm, *Acta Biomaterialia*, 2010, **6**, 2540-2547.
22. H. Bäckdahl, M. Esguerra, D. Delbro, B. Risberg and P. Gatenholm, *Journal of Tissue Engineering and Regenerative Medicine*, 2008, **2**, 320-330.
23. N. Yin, M. D. Stilwell, T. M. A. Santos, H. Wang and D. B. Weibel, *Acta Biomaterialia*, 2015, **12**, 129-138.
24. R. Ravichandran, S. Sundarrajan, J. R. Venugopal, S. Mukherjee and S. Ramakrishna, *Macromolecular Bioscience*, 2012, **12**, 286-311.

25. Q. Xing, F. Zhao, S. Chen, J. McNamara, M. A. DeCoster and Y. M. Lvov, *Acta Biomaterialia*, 2010, **6**, 2132-2139.
26. P. Krontiras, P. Gatenholm and D. A. Hagg, *Journal of Biomedical Materials Research - Part B Applied Biomaterials*, 2014, **103**, 195-203.
27. N. Chiaoprakobkij, N. Sanchavanakit, K. Subbalekha, P. Pavasant and M. Phisalaphong, *Carbohydrate Polymers*, 2011, **85**, 548-553.
28. T. T. Nge, M. Nogi, H. Yano and J. Sugiyama, *Cellulose*, 2010, **17**, 349-363.
29. H. W. Kang, Y. Tabata and Y. Ikada, *Biomaterials*, 1999, **20**, 1339-1344.
30. P. de Oliveira Magalhães, A. M. Lopes, P. G. Mazzola, C. Rangel-Yagui, T. C. V. Penna and A. Pessoa Jr, *Journal of Pharmacy and Pharmaceutical Sciences*, 2007, **10**, 388-404.
31. A. P. Das, P. S. Kumar and S. Swain, *Biosensors and Bioelectronics*, 2014, **51**, 62-75.
32. Q. Fu, C. L. Deng, R. Y. Zhao, Y. Wang and Y. Cao, *Biomaterials*, 2014, **35**, 105-112.
33. K. Su and C. Wang, *Biotechnology Letters*, 2015, **37**, 2139-2145.
34. M. Hornung, M. Ludwig, A. M. Gerrard and H. P. Schmauder, *Engineering in Life Sciences*, 2006, **6**, 546-551.
35. Y. Chen, X. Zhou, Q. Lin and D. Jiang, *Cellulose*, 2014, **21**, 2679-2693.
36. G. Helenius, H. Bäckdahl, A. Bodin, U. Nannmark, P. Gatenholm and B. Risberg, *Journal of Biomedical Materials Research - Part A*, 2006, **76**, 431-438.
37. H. Bäckdahl, G. Helenius, A. Bodin, U. Nannmark, B. R. Johansson, B. Risberg and P. Gatenholm, *Biomaterials*, 2006, **27**, 2141-2149.
38. J. Song, A. Tang, T. Liu and J. Wang, *Nanoscale*, 2013, **5**, 2482-2490.
39. M. A. Alamein, Q. Liu, S. Stephens, S. Skabo, F. Warnke, R. Bourke, P. Heiner and P. H. Warnke, *Advanced Healthcare Materials*, 2013, **2**, 702-717.
40. Z. Li, L. Wang, S. Chen, C. Feng, S. Chen, N. Yin, J. Yang, H. Wang and Y. Xu, *Cellulose*, 2015, **22**, 373-383.
41. G. Guhados, W. Wan and J. L. Hutter, *Langmuir*, 2005, **21**, 6642-6646.
42. S. Yamanaka, K. Watanabe, N. Kitamura, M. Iguchi, S. Mitsuhashi, Y. Nishi and M. Uryu, *Journal of Materials Science*, 1989, **24**, 3141-3145.
43. L. E. Millon and W. K. Wan, *Journal of Biomedical Materials Research - Part B Applied Biomaterials*, 2006, **79**, 245-253.
44. D. Seliktar, *Science*, 2012, **336**, 1124-1128.
45. Y. Lai, A. Asthana and W. S. Kisaalita, *Drug Discov. Today*, 2011, **16**, 293-297.
46. J. Luo and S. T. Yang, *Biotechnology Progress*, 2004, **20**, 306-315.
47. T. Walles, T. Herden, A. Haverich and H. Mertsching, *Biomaterials*, 2003, **24**, 1233-1239.
48. A. Hegen, A. Blois, C. E. Tiron, M. Hellesøy, D. R. Micklem, J. E. Nör, L. A. Akslen and J. B. Lorens, *Journal of Tissue Engineering and Regenerative Medicine*, 2011, **5**, e52-e62.

**Figure captions**

**Fig. 1.** Schematic illustration of template synthesis of Gel/BC. The photograph (a) and SEM (b) image of gelatin microporous template. BC nanofibrils is biosynthesized by *Gluconacetobacter xylinus* in the gelatin microporous template (c). The photograph of resultant Gel/BC scaffold (d).

**Fig. 2.** FE-SEM images and the nanofiber diameter distribution of freeze-dried pure BC. The cross-section of BC pellicle with multilayer structure (a, ×500 magnification) and the porous side (inset, ×2000 magnification); the compact surface of BC pellicle at original magnifications ×10000 (b), ×50000 (inset) and fiber diameter distribution of the BC nanofibrous network (f). The values of average diameter are average ± standard derivation.

**Fig. 3.** FE-SEM images and the diameter distribution of gelatin template and Gel/BC scaffold. The cross-section of gelatin template at original magnifications ×100 (a), ×300 (b) and their micropore diameter distribution (c). The cross-section of Gel/BC scaffold at original magnifications ×100 (d), ×300 (e) and their micropore diameter distribution (f); a micropore of Gel/BC scaffold and surrounding BC nanofibrous network (g); higher magnification of the micropore wall in Gel/BC scaffold (h) and diameter distribution of BC nanofibers (i). The values of average diameter are average ± standard derivation.

**Fig. 4.** ATR-FTIR spectra (a) and XRD patterns (b) of pure BC, gelatin template (Gel) and Gel/BC scaffold.

**Fig. 5.** (a) The mechanical propertiesof pure BC, gelatin template (Gel) and Gel/BC scaffold. (b) Tensile stress-strain curves of Gel and Gel/BC scaffold.

**Fig. 6.** Analysis of ADSCs viability and proliferation on pure BC, gelatin template and Gel/BC scaffolds. (A) 3D LSCM images showing ADSCs viability by Live/dead assay, where live cells fluoresce green and dead calls fluoresce red. Thickness: ≥ 150 μm. (B) Viability of seeded ADSCs in the scaffolds with the cultivation of 1, 7 and 14 days. (C) Number of ADSCs after proliferation on scaffolds for 1, 7 and 14 days cell culture.

**Fig. 7.** Scaffold architecture and cell binding for pure BC (a), gelatin template (b) and Gel/BC scaffold (c). Interaction between cells and BC nanofibers (d). FE-SEM images of ADSCs attachment on the three scaffolds after 24 h cultivation. Images of ADSCs on the BC compact surface at original magnifications ×1000 (e), ×20000 (e inset). The cross-section of gelatin template at original magnifications ×1000 (f), ×3000 (f inset). The cross-section of Gel/BC scaffold at original magnifications ×1000 (g), ×3000 (g inset).

**Fig. 8.** The photograph and histologic analysis of subcutaneously implanted scaffolds at 2 weeks with hematoxiylin-eosin (H&E), Masson's trichrome staining (Masson), and CD31 staining for detection of revascularization, immunohistochemical staining of T-cell specific antibody (CD3), B-cell specific antibody (CD22) and macrophage-specific antibody (CD68) were used to identify the inflammatory cells. Bar scales: 100 μm.

**Fig. 1.**

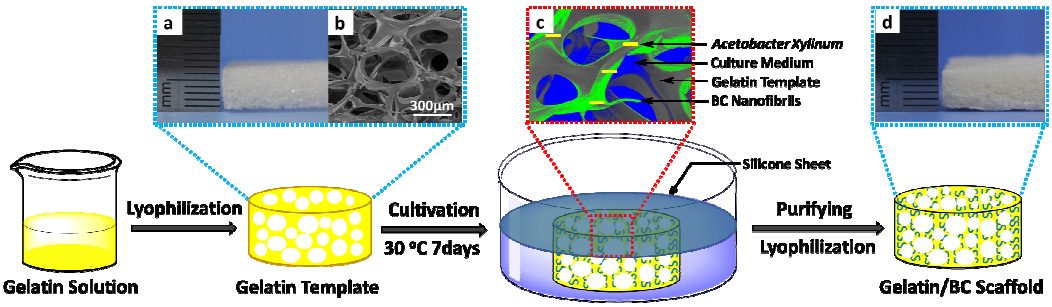

**Fig. 2.**

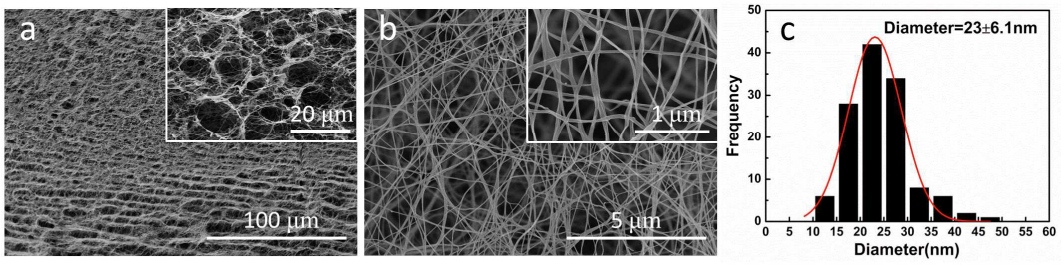

**Fig. 3.**

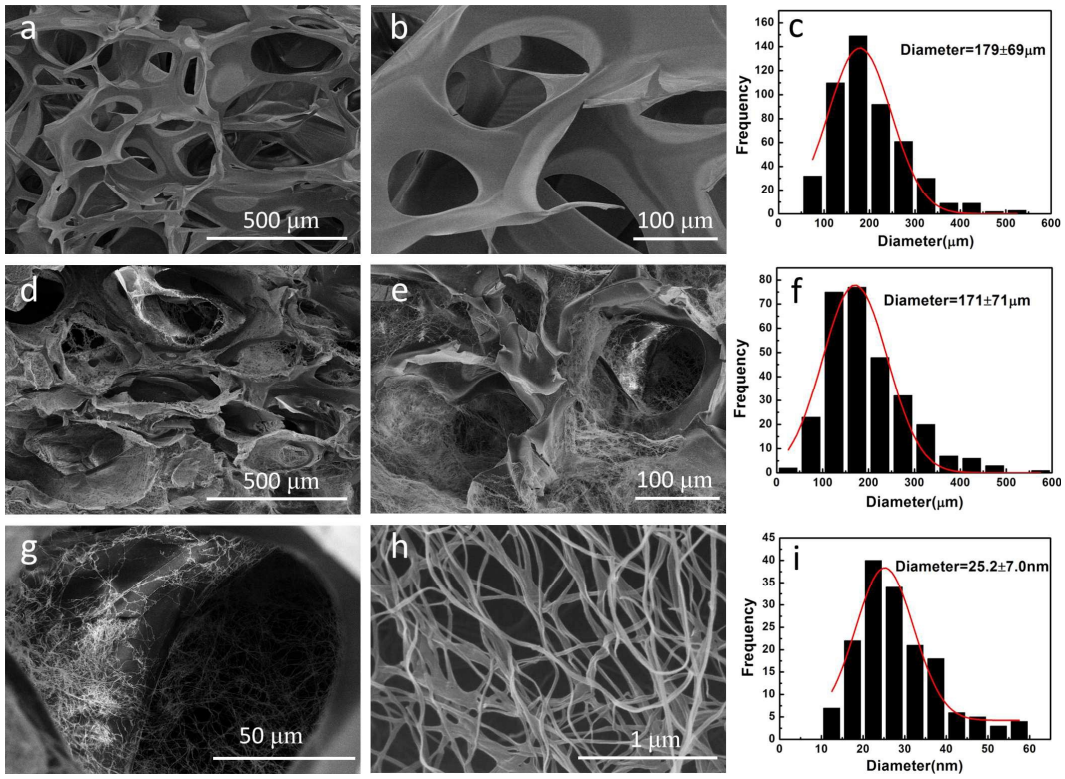

**Fig. 4.**

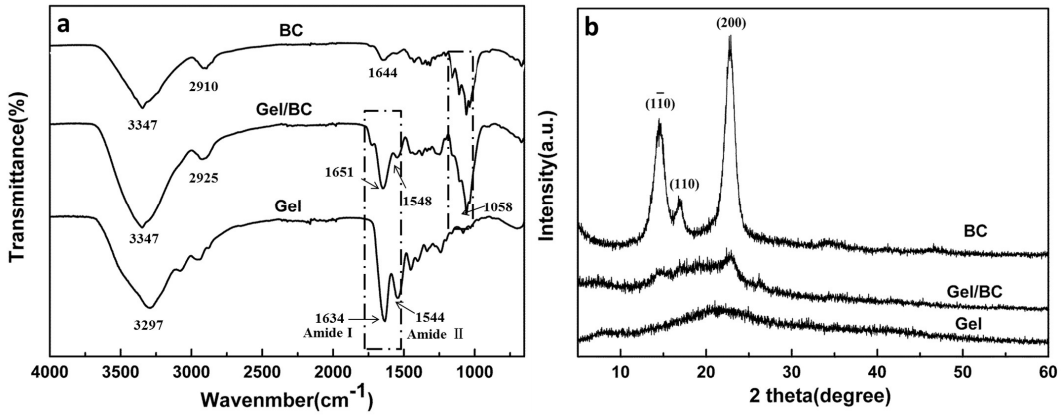

**Fig. 5.**

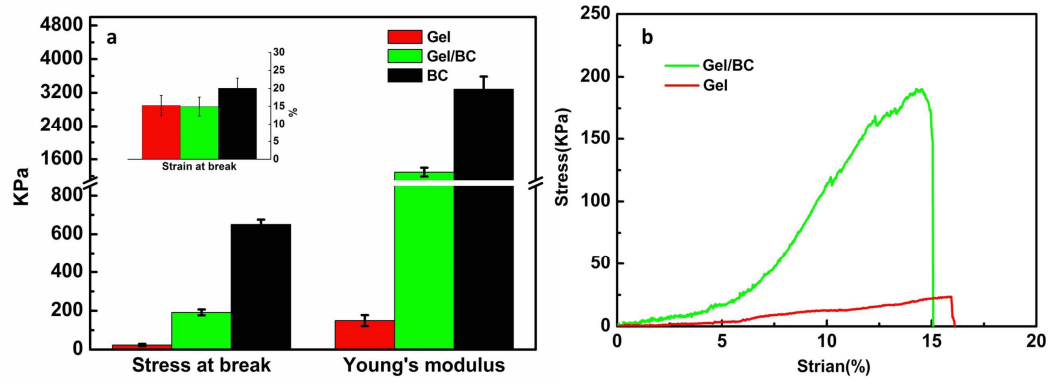

**Fig. 6.**

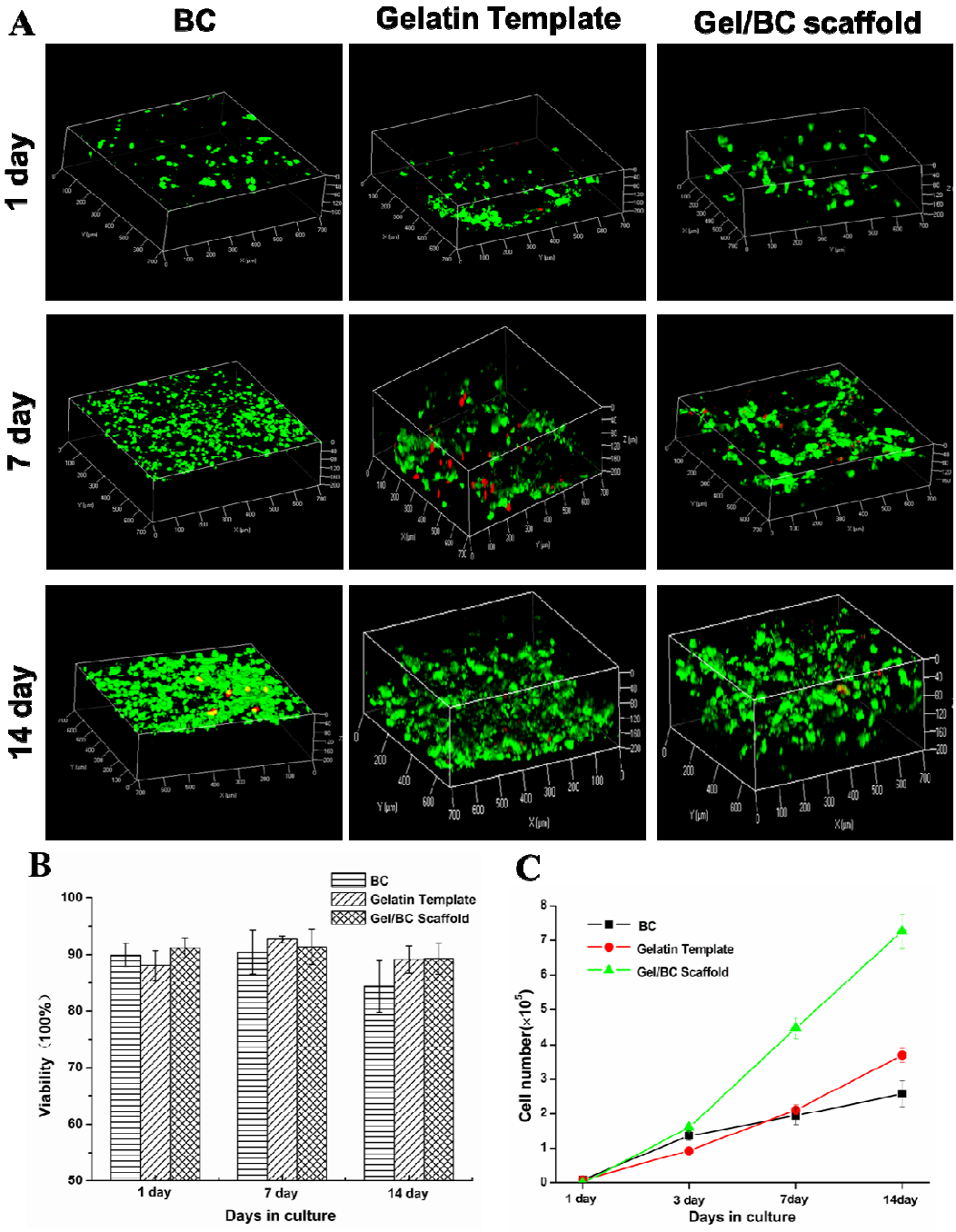

**Fig. 7.**

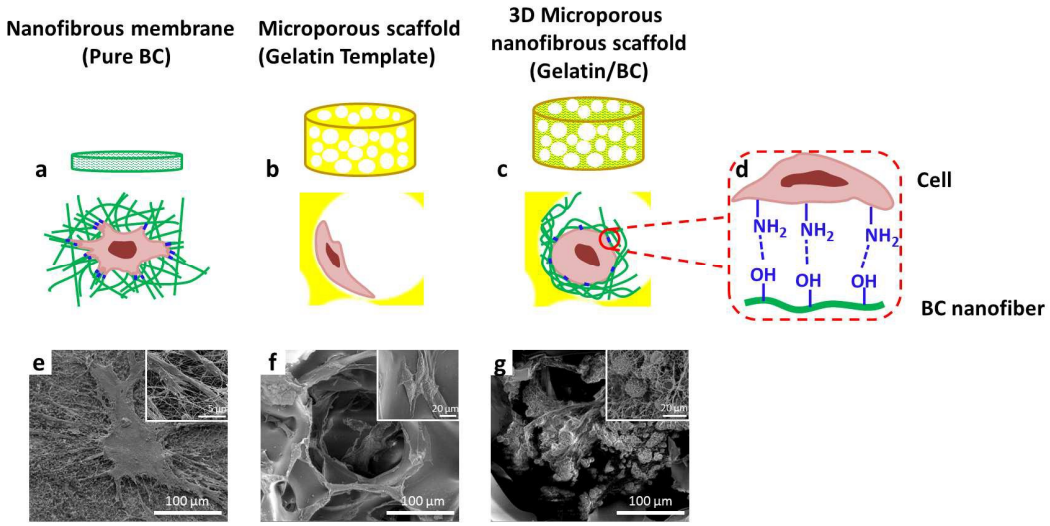

**Fig. 8.**

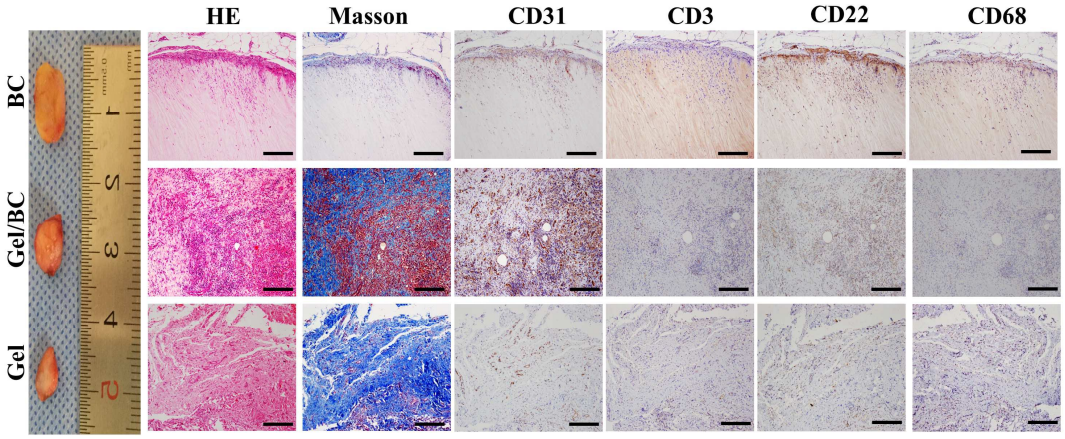

# Graphical abstract

## Improved cell infiltration and vascularization of three-dimensional bacterial cellulose nanofibrous scaffolds by template biosynthesis

Zhe Li[a,Ψ], Xiangguo LV[b,Ψ], Shiyan Chen[a]*, Baoxiu Wang[a], Chao Feng[b]*, Yuemin Xu[b], Huaping Wang [a]*

[a] State Key Laboratory for Modification of Chemical Fibers and Polymer Materials, Key Laboratory of Textile Science & Technology (Ministry of Education), College of Materials Science and Engineering, Donghua University, Shanghai, 201620, People's Republic of China

E-mail: chensy@dhu.edu.cn, wanghp@dhu.edu.cn

Tel: +86-21-67792958, fax: +86-21-67792950

[b]Department of Urology, Affiliated Sixth People's Hospital, Shanghai Jiaotong University, Shanghai, 200233, People's Republic of China

E-mail: engchaomed@sina.com

Tel: +86-21-64369181, fax: 86-21-64083783

[Ψ]Co-first author: These authors contributed equally to the work.